

Figure 2. Schematic reaction coordinate for ligand dissociation in ML_5 complexes. (The curves do not necessarily have to have minima in the middle, particularly if the coordinate for intramolecular exchange alone has no minimum.) A family of curves is shown which semiquantitatively represent the situation for RhL_5 complexes: a, $L = P(O-n-C_4H_9)_3$; b, $L = P(O-n-C_3H_7)_3$; c, $L = P(OC_2H_5)_3$; d, $L = P(OCH_3)_3$.

remain collinear throughout the dissociative reaction. A family of schematic free energy changes is shown in Figure 2, assuming the intermediate (or transition state) for intramolecular exchange also occurs on the reaction coordinate for ligand dissociation. This tetragonal-pyramidal geometry occurs near one vertical dotted line in the figure—to the left if there is no minimum in the reaction coordinate for intramolecular exchange, to the right if there is. Intramolecular exchange can be effected by population of the tetragonal-pyramidal state followed by return to a rearranged trigonal bipyramid. Both $\Delta G^*(intra)$ and $\Delta G^*(inter)$ are well-defined maxima in the ligand dissociation reaction coordinate (Figure 2). The geometrical correspondence between Figures 1 and 2 is shown by the symbols TBP, TP, TP', SP, and L.

Table I shows that while $\Delta G^*(intra)$ increases with increasing steric bulk of the ligand for RhL_5^+ compounds due to steric crowding of the tetragonal pyramid relative to the trigonal bipyramid,⁴ the corresponding $\Delta G^*(inter)$ values are almost constant. The invariance of $\Delta G^*(inter)$ to alkyl phosphite size may be interpreted as the cancellation of two steric effects: one, the sterically unfavorable effect of crowding of the basal ligands in the TP intermediate; two, the steric assistance to axial bond breaking in TP'. These two steric effects nearly cancel and the resulting invariance of $\Delta G^*(inter)$ reflects the very similar electronic properties of the ligands. $\Delta\Delta G^* = \Delta G^*(inter) - \Delta G^*(intra)$ and is a rough measure of the free energy necessary to break the axial bond in TP. Figure 2 shows a set of semiquantitative reaction coordinates for the RhL_5^+ complexes. Curves are normalized to coincide at the TBP point. The SP + L section, unlike the rest of the curve, is likely to be quite sensitive to solvent; the equilibrium constant for dissociation [a function of $G(P + L) - G(TBP)$] increases as the steric bulk of L increases, making curve (a) the lowest at the SP + L position.

Acknowledgment. We gratefully acknowledge the skilled technical assistance of G. Watunya and M. A. Cushing.

Registry No. $Co[P(OC_2H_5)_3]_5^+$, 58448-89-8; $Ir[P(OC_2H_5)_3]_5^+$, 53701-79-4; $Ni[P(OC_2H_5)_3]_5^{2+}$, 58448-90-1; $Pt[P(OC_2H_5)_3]_5^{2+}$, 53659-72-6; $Pd[P(OC_2H_5)_3]_5^{2+}$, 53701-83-0; $Rh[P(OCH_3)_3]_5^+$, 48077-64-1; $Rh[P(OC_2H_5)_3]_5^+$, 51153-38-9; $Rh[P(O-n-C_3H_7)_3]_5^+$, 58448-91-2; $Rh[P(O-n-C_4H_9)_3]_5^+$, 51153-36-7; $Rh[P(OCH_2)_3CCH_3]_5^+$, 51153-39-0.

References and Notes

- (1) J. Powell and D. G. Cooper, *J. Chem. Soc., Chem. Commun.*, 749 (1974), and earlier references.
- (2) D. A. Redfield and J. H. Nelson, *J. Am. Chem. Soc.*, **96**, 6219 (1974), and earlier references.
- (3) (a) L. Cattalini, *MTP Int. Rev. Sci.: Inorg. Chem., Ser. One*, **9**, 269 (1972); (b) C. H. Langford and H. G. Gray, "Ligand Substitution Processes", W. A. Benjamin, New York, N.Y., 1966.
- (4) J. P. Jesson and P. Meakin, *J. Am. Chem. Soc.*, **96**, 5760 (1974), and earlier references.
- (5) R. S. Berry, *J. Chem. Phys.*, **32**, 933 (1960).
- (6) E. L. Muetterties and L. J. Guggenberger, *J. Am. Chem. Soc.*, **96**, 1748 (1974).
- (7) K. N. Raymond, P. W. R. Corfield, and J. A. Ibers, *Inorg. Chem.*, **7**, 1362 (1968).
- (8) P. Meakin, R. A. Schunn, and J. P. Jesson, *J. Am. Chem. Soc.*, **96**, 277 (1974); A. D. English, P. Meakin, and J. P. Jesson, *ibid.*, **98**, 422 (1976).
- (9) Tetragonal-pyramidal geometries possessing C_{4v} symmetry seem quite likely for the present case where all ligands are identical. In the case where all ligands are not the same, a geometry of lower symmetry considering only bond angles and lengths (not the difference of the substituents) would be expected.

Contribution from the Institut für Anorganische Chemie der Universität Frankfurt, D-6 Frankfurt/M 70, West Germany, the Institut für Anorganische Chemie der Universität Karlsruhe, D-75 Karlsruhe 1, West Germany, and the Institut für Theoretische Chemie der Universität Düsseldorf, D-4 Düsseldorf, West Germany

Photoelectron Spectra of Group 5 Compounds. II.¹ Conformational Analysis of Diphosphine (P_2H_4)

Susanne Elbel,* Heindirk tom Dieck, Gerd Becker, and Walther Ensslin

Received September 15, 1975

AIC50682T

The photoelectron spectra of certain hydrazines,²⁻⁴ disulfides,⁵ peroxides,⁶ and aminophosphines^{7,8} have been assigned to a unique conformer, being present under normal PE spectroscopic conditions. In contrast, different rotamers could be detected in the PE spectra of hexahydropyridazines^{3b} and tetrasubstituted diphosphines and diarsines⁹ and were assumed for polysilanes.¹⁰ The composition of the rotameric mixture (trans:gauche) obtained for tetramethyldiphosphine from the relative PE peak areas⁹ had to be revised.¹¹

For the simplest diphosphine P_2H_4 structural data^{12,13} and the results from ab initio¹⁴ and semiempirical¹⁵ methods are available which are consistent with preponderant gauche conformation. However, some discrepancies remain in the reported equilibrium dihedral angles, barrier magnitudes, or the amount of trans isomers. Therefore, it was of interest to elucidate the structure of P_2H_4 by PE spectroscopy.¹⁶ To gain some insight into its conformational composition we tried to simulate the experimental PE spectrum of P_2H_4 with EHMO, CNDO, and the reported ab initio orbital energies.^{14,17a}

Experimental Section and Computational Details

The He I (584-Å) PE spectra were recorded with a Perkin-Elmer PS 16 spectrometer and calibrated with argon (resolution 35–40 meV).

Diphosphine was prepared as described by Baudier and Schmidt,¹⁸ by treating calcium phosphide (Riedel de Haen AG, Seelze) with water in a high-vacuum line, followed by purification by trap to trap distillation.

To retard decomposition, giving PH_3 and solid polymers P_nH_n , catalyzed by traces of acids, a continuous flow of ammonia was passed through the PE spectrometer and the inlet equipment over a period of 24 h before the actual measurements. To maintain a constant

* To whom correspondence should be addressed at the Institut für Anorganische Chemie der Universität Frankfurt.

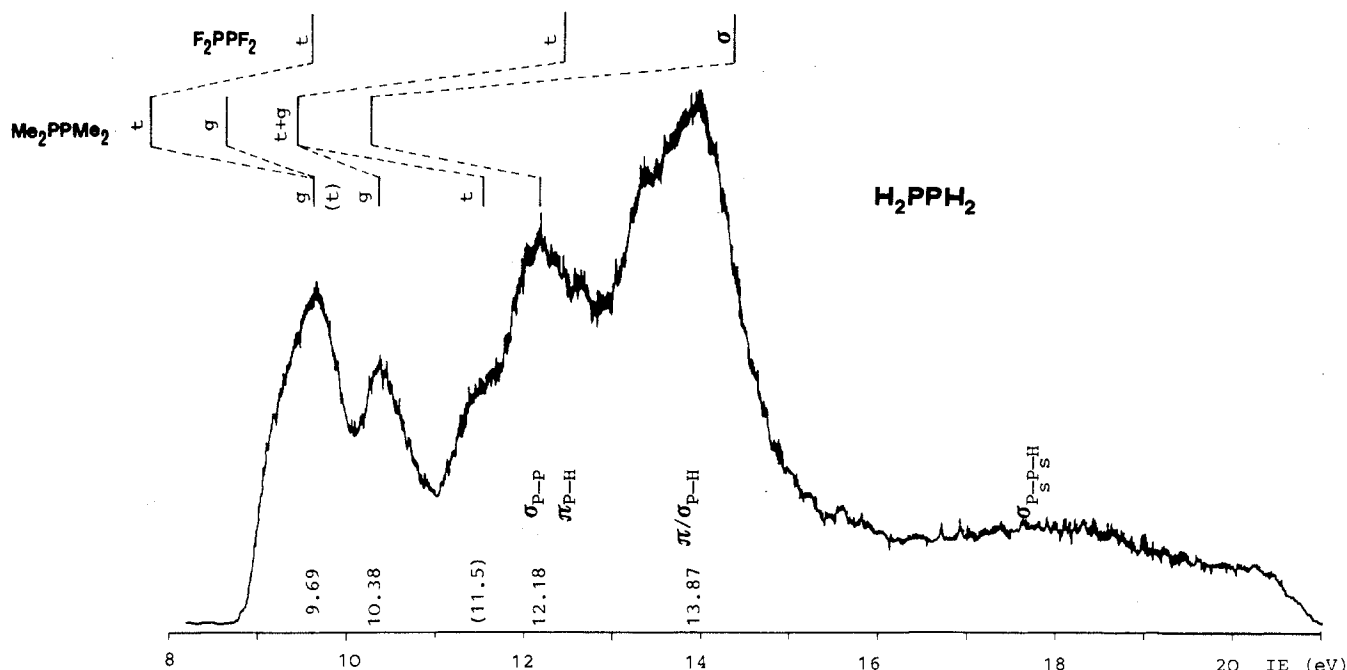


Figure 1. PE spectrum and vertical IP's of diphosphine as well as vertical lone-pair ionization energies of P_2Me_4 and P_2F_4 .

pressure during the recordings P_2H_4 was immersed in a CO_2 -ether cooling mixture and was stirred magnetically. The more volatile PH_3 which was clearly distinguishable by its characteristic first band exhibiting vibrational fine structure could be completely removed in this way after 2 h. Several spectra were then run within a period of 12 h. No changes in band shapes could be detected. (This contrasts P_2Me_4 where contaminating PMe_3 discernible by changes in band intensities could not be removed entirely within 12 h despite repeated fractional distillation. The first PE band of PMe_3 (8.6 eV¹) coincides with the second band of P_2Me_4 obscuring its real intensity!)

CNDO (with and without d orbitals) and EHMO calculations (without d orbitals) were performed on the Univac 1108 computer of the University Computing Center at Frankfurt/M.

Phosphorus 3p and 3s valence ionization potentials were parametrized in the EHMO computations of PH_3 in order to reproduce the experimental n/σ energy gap (ca. 3 eV) within the corresponding eigenvalues. The parameters thus obtained (P_{3p} , 11.0 eV; P_{3s} , 19.0 eV) were employed in EHMO calculations of P_2H_4 to gain a reasonable energy separation $\Delta E(n \leftrightarrow \sigma)$.

Ab initio eigenvalues were estimated from the orbital energy plot presented by Van Wazer et al.¹⁴ Their ab initio and CNDO total energy equations have been used too.

The simulation of the PE spectrum of P_2H_4 was carried out using our "Boltzmann" program previously described.¹⁰ Lorentz curves instead of Gaussians were chosen since they fitted slightly better experimental band contours. No significant changes in the simulated spectra have been detected on varying T from -30 to $+30$ °C in the Boltzmann expression, considering possible Joule-Thompson effects. The different bonding characters of the σ_{P-H} and n_P lone-pair orbitals were taken into account reducing the half-widths of n_P bands by a factor of 0.67 with respect to σ bands (half-width 0.7 eV). s-Type orbitals (1a, 1b) and the instrumental decrease in intensity occurring at higher energies were neglected.

The orbital and total energies of P_2H_4 were calculated by varying only the twist angle ϕ from 0° (cis, eclipsed) to 180° (trans, staggered) at intervals of 10°.

Results and Discussion

The He I PE spectrum of diphosphine is given in Figure 1. Six of seven bands due to valence orbitals are expected according to corresponding ab initio¹⁴ and semiempirical calculations. Weak bands beyond 15.5 eV (ca. 18 and 20.3 eV) should be due to P_s-H (1b) and $(H)P_s-P_s(H)$ (1a) σ -bonding levels. Between 12 and 15.5 eV two partly overlapping bands of different intensity due to σ_{P-P} (3a) and σ/π_{P-H} (2a, 2b) levels occur. The low-energy shoulder at 11.5 eV is attributed

to the trans lone-pair orbital combination n_+ if analogy with P_2Me_4 ^{9,16} and P_2F_4 ¹⁹ PE data is assumed (Figure 1). Below 11 eV the P_2H_4 spectrum contains two lone-pair bands centered at 9.69 and 10.38 eV. The first one is assigned mainly to the gauche combination n_- (4a). It exhibits a shoulder on its low-energy side indicating another conformational ratio than in perfluoro- and permethyldiphosphine. Their lone-pair bands are nearly symmetrical and were assigned to only one or two fixed molecular geometries, respectively. The second band is attributed to the gauche combination n_+ (3b) and should not be confused with the first band of PH_3 (10.59 eV)²⁰ (see Experimental Section).

Although the gauche configuration is predicted to be the most stable one of diphosphine,^{12,14,15} it is known that barriers to rotation around P-P bonds are much smaller than in hydrazines (e.g., see ref 17), and should favor the population of different rotamers. Our simulation includes total energy curves ($\phi = 0 \rightarrow 180^\circ$) with a Boltzmann distribution at 25 °C using the calculations cited above.

Barrier curves and eigenvalue plots are compared in Figure 2. Corresponding simulated PE spectra are obviously governed by energy sets at their equilibrium dihedral angles.

Graphs of EHMO eigenfunctions for the eclipsed (0°, C_{2v}) and staggered (180°, C_{2h}) rotamers of P_2H_4 are displayed in Figure 3 to illustrate n , σ , and π symbols used here to characterize the main orbital contributions.

Although the experimental band contours are badly reproduced by all calculations employed here, the best agreement between experimental and simulated PE spectra is provided by the ab initio method.¹⁴ The spectrum in Figure 2 A clearly shows that the main component of both separated lone pairs found experimentally (9.69 and 10.38 eV) originates from the gauche split. The trans rotamer is calculated to be present with ~10% only. The conclusion of Ames and Turner that n_\pm orbital energies of the gauche conformation of P_2Me_4 are separated¹¹ is substantiated by our observation. The Δn_P energy gap (Figure 1, 0.69 eV) is similar to that in hydrazine (0.73 eV);²⁻⁴ this is unexpected since orbital interactions should be comparatively smaller with longer bonds.

The unsuccessful simulation by semiempirical techniques can be understood from Figure 2. Although the overall eigenvalue plots are rather similar, the ϕ -dependent total energy

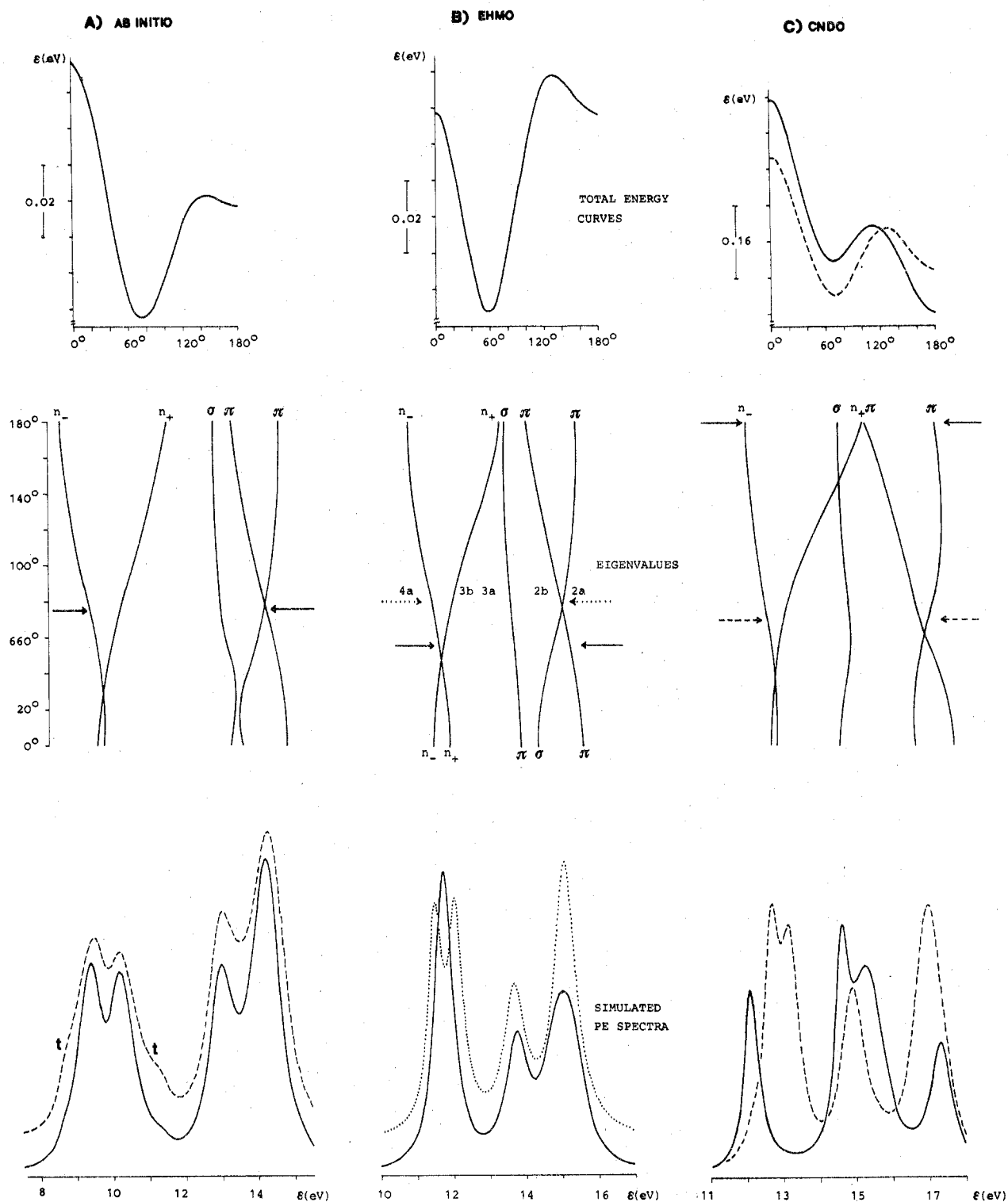


Figure 2. Comparison of total energy curves, eigenvalue plots, and simulated PE spectra of P_2H_4 from (A) ab initio,¹⁴ (B) EHMO (—d), and (C) CNDO (+d) calculations. Equilibrium angles are indicated by arrows within the eigenvalue plots. The dotted lines refer (A) to an ab initio barrier curve compressed by an energy scale factor of 0.6, (B) to simulation with $\phi = 80^\circ$, and (C) to simulation based on Van Wazer's CNDO (+d) total energy equation.

curves disagree either in minimum angles or in the barrier heights. While the ab initio equilibrium angle (75.2° ¹⁴ (75°), 180° ^{17a}) is close to the experimental one (74° ,¹² 81° ¹³), EHMO calculations favor a total energy minimum with ϕ approximately 58° , here np energies being almost degenerate. Better simulation from EHMO data is obtained using the experimental ϕ angle (Figure 2B, dotted line, 80°). The CNDO total energy curve (Figure 2C, solid line) favors staggered rotamers similar to Wagner's ab initio barrier curve

and is therefore unrealistic. Van Wazer's CNDO (+d) total energy equation referring to another set of parameters gives a much better fit (Figure 2C, broken line) confirming the assumption of predominant gauche rotamers.

Comparing the vertical np IP's of P_2Me_4 ⁹ and P_2F_4 ¹⁹ with those of P_2H_4 (Figure 1) and especially analyzing the shapes of the first and the third bands there is good reason for trans conformers being present to a larger extent as is suggested by the "arrest" at 180° of the ab initio barrier curve (Figure 2A).

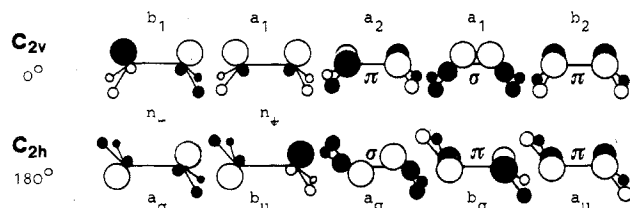


Figure 3. EHMO orbital diagrams and their irreducible representations in C_{2v} (eclipsed) and C_{2h} (staggered) of P_2H_4 .

Therefore we artificially compressed this curve with an energy scale factor of 0.6 to increase the population of trans species. The resulting simulated spectrum is shown in Figure 2A as a broken line, and bands attributed to the trans isomers are indicated "t".

Assuming an approximately parallel shift of lone-pair energies upon replacement of H by methyl groups (compare to N_2H_4 , N_2Me_4 ²⁻⁴) or by F atoms (the perfluoro effect should equalize Δn_p gaps of "trans-only" P_2H_4 and P_2F_4 molecules due to pseudo- π symmetry, C_{2h}), the $n_+(t)$ combination of trans-diphosphine is assigned to the band at 11.5 eV overlapped by σ - and π -orbital ionizations. The $n_-(t)$ combination is then responsible for the low-energy asymmetry of the first band (Figure 1).

It seems that the sufficient separation of lone-pair ionization energies of different rotamers makes diphosphine a good example for making PE studies of temperature-dependent changes in conformer populations as well as for checking the quality of computed rotational barriers.

Registry No. P_2H_4 , 13445-50-6.

References and Notes

- (1) Part I: S. Elbel, H. Bergmann, and W. Ensslin, *J. Chem. Soc., Faraday Trans. 2*, **70**, 555 (1974).
- (2) K. Osafune, S. Katsumata, and K. Kimura, *Chem. Phys. Lett.*, **19**, 369 (1973).
- (3) (a) S. F. Nelsen and J. M. Buschek, *J. Am. Chem. Soc.*, **95**, 2011 (1973); (b) *ibid.*, **95**, 2013 (1973); (c) *ibid.*, **96**, 2393 (1974).
- (4) P. Rademacher, *Chem. Ber.*, **108**, 1548, 1557 (1975), and literature quoted therein.
- (5) (a) A. D. Baker, M. Brisk, and M. Gellender, *J. Electron Spectrosc.*, **3**, 227 (1974); (b) G. Wagner and H. Bock, *Chem. Ber.*, **107**, 68 (1974); (c) C. Guimon, M. C. Guimon, and G. Pfister-Guillouzo, *Tetrahedron Lett.*, **441**, 1413 (1975).
- (6) (a) K. Osafune and K. Kimura, *Chem. Phys. Lett.*, **25**, 47 (1974); (b) C. Batich and W. Adam, *Tetrahedron Lett.*, **1467** (1974); (c) D. W. Davies, *Chem. Phys. Lett.*, **28**, 520 (1974).
- (7) A. H. Cowley, M. J. S. Dewar, D. W. Goodman, and J. R. Schweiger, *J. Am. Chem. Soc.*, **95**, 6506 (1973).
- (8) A. H. Cowley, M. J. S. Dewar, J. W. Gilje, D. W. Goodman, and J. R. Schweiger, *J. Chem. Soc., Chem. Commun.*, **340** (1974).
- (9) A. H. Cowley, M. J. S. Dewar, D. W. Goodman, and M. C. Padolina, *J. Am. Chem. Soc.*, **96**, 2648 (1974).
- (10) W. Ensslin, H. Bergmann, and S. Elbel, *J. Chem. Soc., Faraday Trans. 2*, **71**, 913 (1975).
- (11) D. L. Ames and D. W. Turner, *J. Chem. Soc., Chem. Commun.*, **179** (1975).
- (12) J. R. Durig, L. A. Carreira, and J. D. Odom, *J. Am. Chem. Soc.*, **96**, 2688 (1974).
- (13) B. Beagley, A. R. Conrad, J. M. Freeman, J. J. Monaghan, B. G. Norton, and G. C. Holywell, *J. Mol. Struct.*, **11**, 371 (1972).
- (14) (a) I. Absar, J.-B. Robert, and J. R. Van Wazer, *J. Chem. Soc., Faraday Trans. 2*, **68**, 799 (1972); (b) *Chem. Commun.*, **356** (1970).
- (15) (a) A. H. Cowley, W. D. White, and M. C. Damasco, *J. Am. Chem. Soc.*, **91**, 1922 (1969); (b) K. Issleib and W. Gröndler, *Theor. Chim. Acta*, **11**, 107 (1968); (c) A. H. Cowley and W. D. White, *J. Am. Chem. Soc.*, **91**, 1917 (1969).
- (16) S. Elbel, Ph.D. Thesis, University of Frankfurt/M, 1974.
- (17) (a) E. L. Wagner, *Theor. Chim. Acta*, **23**, 127 (1971); (b) *ibid.*, **23**, 115 (1971).
- (18) M. Baudler and L. Schmidt, *Z. Anorg. Allg. Chem.*, **289**, 219 (1957).
- (19) S. Craddock and D. W. H. Rankin, *J. Chem. Soc., Faraday Trans. 2*, **68**, 940 (1972).
- (20) (a) G. R. Branton, D. C. Frost, C. A. McDowell, and I. A. Stenhouse, *Chem. Phys. Lett.*, **5**, 1 (1970); (b) A. W. Potts and W. C. Price, *Proc. R. Soc. London, Ser. A*, **326**, 181 (1972).

Contribution from the Department of Chemistry, McMaster University, Hamilton, Ontario, Canada L8S 4M1, and the Materials Research Laboratory, The Pennsylvania State University, University Park, Pennsylvania 16802

Magnetic Properties of the Divalent Europium Scheelites $EuMoO_4$ and $EuWO_4$ and the Mixed-Valence Phases Eu_xMoO_4 and Eu_xWO_4

J. E. Greedan,* Richard G. Johnston, and Gregory J. McCarthy

Received December 2, 1975

AIC50868S

Previous reports of the magnetic behavior of the scheelite phase $EuWO_4$ are in conflict. Shafer¹ observed paramagnetic behavior down to 1.6 K with $\Theta_c = 0$ K but few details are given. Houlihan et al.² have reported some evidence of magnetic ordering with $\Theta_c = +18$ K. We have restudied the magnetic properties of $EuWO_4$ and the isostructural molybdate, $EuMoO_4$, in an effort to clarify the situation.

Included in our study are some members of the closely related phases Eu_xMO_4 representing solid solution between $EuMO_4$ and $Eu_2(MO_4)_3$ ($Eu_{0.667}MO_4$, $M = W, Mo$) reported recently by Nemiroff and Banks³ and Johnston and McCarthy.⁴ These phases represent a unique type of mixed-valence europium oxide in which divalent and trivalent europium ions apparently occupy the same crystallographic site in the scheelite lattice. According to the criteria of Robin and Day⁵ the existence of two different oxidation states of the same element in crystallographically equivalent sites leads to extensive electron-transfer effects between the ions. Compounds containing such species are predicted to have high electrical conductivities, strong magnetic exchange effects, and intense optical bands not present in the spectra of the isolated ions themselves (class IIIB behavior). On the other hand if the site coordination of the two ions is slightly different, i.e., different metal-ligand bond lengths, the electron-transfer effects are expected to be more limited but still discernible (class II behavior). It is of some interest to apply these criteria to the Eu_xMO_4 phases.

Experimental Section

Preparation of Compounds. The compounds were prepared as described in previous reports.⁴ Briefly, for $EuMO_4$ and $Eu_2(WO_4)_3$ the starting materials consisted of appropriate weights of reagent grade oxides, powdered metals, and carbonates which were mixed, pelletized, and fired at 1050 °C for 48–130 h. The solid solutions were prepared by direct reaction between end members. Phases involving divalent europium were fired in sealed silica tubes at a low pressure of 10^{-3} Torr.

Magnetic Measurements and Diffuse Reflectance Spectra. Magnetic data were collected using a PAR vibrating-sample magnetometer over the temperature range from 1.2 to 300 K. Calibration was done using $Hg(Co(SCN)_4)$ and a small sphere of high-purity nickel. Samples consisted of pressed or sintered disks attached to the vibrating rod using low-temperature varnish.

Diffuse reflectance spectra were obtained using a Beckman DK-2A equipped with an integrating sphere and a $BaSO_4$ standard.

Results and Discussion

$EuWO_4$ and $EuMoO_4$. Results of susceptibility measurements were analyzed in terms of the Curie-Weiss Law. Molar Curie constants, C_M , were found to be 7.74 and 7.79 for $EuWO_4$ and $EuMoO_4$, respectively. Note that the Curie constants are slightly less than the theoretical value, 7.87, indicating minor contamination by Eu^{3+} leading to actual compositions of $Eu_{0.99}WO_4$ and $Eu_{0.99}MoO_4$. In contrast to previous reports $\Theta_c = -5$ K for both compounds suggesting the possibility of antiferromagnetic exchange. As shown in Figure 1 (inset) no evidence of a Neel point can be observed

* To whom correspondence should be addressed at McMaster University.